Heterogeneous & Homogeneous & Bio- & Nano-

CHEMCATCHEM

CATALYSIS

Accepted Article

Title: Solution Synthesis of N,N-Dimethylformamide-stabilized Iron Oxide Nanoparticles as an Efficient and Recyclable Catalyst for Alkene Hydrosilylation

Authors: Ryusei Azuma, Seiya Nakamichi, Jungo Kimura, Hiroki Yano, Hideya Kawasaki, Takeyuki Suzuki, Ryota Kondo, Yasuharu Kanda, Ken-ichi Shimizu, Kazuo Kato, and Yasushi Obora

To be cited as: *ChemCatChem* 10.1002/cctc.201800161

Link to VoR: http://dx.doi.org/10.1002/cctc.201800161

A Journal of

ChemPubSoc Europe

WILEY-VCH

www.chemcatchem.org

ChemCatChem 10.1002/cctc.201800161

Solution Synthesis of *N*,*N*-Dimethylformamide-stabilized Iron Oxide Nanoparticles as an Efficient and Recyclable Catalyst for Alkene Hydrosilylation

Ryusei Azuma,[a] Seiya Nakamichi,[a] Jungo Kimura,[a] Hiroki Yano,[a] Hideya Kawasaki,[a] Takeyuki Suzuki,[b] Ryota Kondo,[a] Yasuharu Kanda,[c] Ken-ichi Shimizu,[d] Kazuo Kato[e] and Yasushi Obora*[a]

Dedication ((optional))

Abstract: *Highly activated, monodisperse N,N-dimethylformamide (DMF)-stabilized iron oxide nanoparticles (Fe_2O_3 NPs) were synthesized using Iron(III) acethylacetonate as a precursor under open air conditions. The resulting Fe_2O_3 NPs were characterized using various techniques (e.g. TEM, DLS, XRD, XPS, FT-IR, XANES). The Fe_2O_3 NPs exhibited efficient catalytic activity for the hydrosilylation of alkenes, without the need for further additives. Effective recycling process of the colloidal catalyst by extraction with a hexane-DMF system was developed and multiple recycles of the catalyst resulted in no significant loss of catalytic activity at least five times.*

Abundant transition metals, such as Fe, Co and Ni, are being used increasingly frequently in catalysis as alternatives to rarer metals. Various organic syntheses using more widely available metal catalysts have been reported.[1] In particular, iron catalysts have shown significant utility because they are inexpensive, abundant in the earth, easy to handle and exhibit low toxicity. As a result, they are currently being developed for general catalytic reactions such as cross-coupling, cycloadditions and polymerizations.[2]

Organosilicon compounds are important intermediates in various materials science, and are also used as reagents for fine chemical synthesis.[3,4] Preparation of organosilicon compounds therefore has high industrial value. A versatile reaction introducing silicon groups into organic compounds has been studied and is receiving significant attention.[5] Hydrosilylation of alkenes is regarded as an efficient method of obtaining organosilicon compounds.[6] Traditionally, platinum complexes such as Speier's[7] and Karstedt's[8] catalysts served as efficient catalysts for hydrosilylation of alkenes in the silicone chemical industry. However, although platinum has high catalytic activity, it has some limitations, such as being a rare metal, as well as its tendency to induce side reactions. In 2004, Chirik and co-workers reported a well-designed iron-pincer type catalyst, which shows remarkable activities in the hydrosilylation of alkenes and alkynes.[9] However, the pre-catalysts are sensitive to air and moisture, and therefore need careful preparation. Following the report by Chirik, iron catalyst systems with organometallic co-catalysts as activators, such as EtMgBr and $NaBHEt_3$, were reported.[10] Recently, Nagashima and co-workers reported iron and cobalt complex-catalyzed hydrosilylation of alkenes with alkyl isocyanides as ligands.[11] Iron catalysts activated by alkylamines, such as $(iPr)_2NEt$ or Et_3N were also used for hydrosilylation of alkenes or alkynes.[12] Others have also developed Ni and Co catalysts, which provided practical approaches to catalytic hydrosilylation.[6c, 6d, 13]

Transition metal nanoparticles possess various specific properties, which have been utilized across a wide range of applications in biology, pharmaceuticals, electronics and catalysis, amongst others.[14] In particular, considerable attention has been focused on nanoparticle catalysts.[15] Metal nanoparticles have been expected to show enhancement of catalytic activity and low catalyst loading as a result of their increased surface area compared with the bulk metal. In general, metal nanoparticles are synthesized by the liquid phase reduction method, which requires reducing and protecting agents.[16] Our group has reported a simple preparation method for DMF-stabilized metal nanoparticles (Pd, Pt, Ir and Cu) using the DMF reduction method.[17] Since DMF was both the reducing and protecting agent, metal nanoparticles were easily synthesized in a one step process and the resulting nanoparticles provided sufficient catalytic activity for organic synthesis. Pd nanoclusters (NCs) with a particle size of 1–2 nm, have been demonstrated as a practical and recyclable catalyst for Suzuki-Miyaura, Mizoroki-Heck and Migita-Kosugi-Stille reactions.[17a,17b] Cu NPs can be used for Sonogashira coupling and *O*-arylation[17c,17d] and Ir NCs catalyze β-methylation of alcohols through hydrogen autotransfer.[17e]

---

[a] R. Azuma, S. Nakamichi, J. Kimura, H. Yano, Prof. Dr. H. Kawasaki, Dr. R. Kondo, Prof. Dr. Y. Obora
Department of Chemistry and Materials Engineering, Faculty of Chemistry, Materials and Bioengineering, Kansai University, Suita, Osaka 564-8680 (Japan)
E-mail: obora@kansai-u.ac.jp
[b] Prof. Dr. T. Suzuki
Comprehensive Analysis Center, The Institute of Scientific and Industrial Research (ISIR), Osaka University, 8-1 Mihogaoka, Ibaraki, Osaka 567-0057 (Japan)
[c] Dr. Y. Kanda
Applied Chemistry Research Unit, Collage of Environmental Technology, Graduate School of Engineering, Muroran Institute of Technology, 27-1 Mizumoto, Muroran 050-8585 (Japan)
[d] Prof. Dr. K.-i. Shimizu
Institute for Catalysis, Hokkaido University, N-21, W-10, Sapporo 001-0021 (Japan)
[e] Dr. Kazuo Kato
Japan Synchrotron Radiation Research Institute, 1-1-1 Kouto, Sayo-cho, Sayo-gun, Hyogo 679-5198 (Japan)

Supporting information for this article is given via a link at the end of the document.

10.1002/cctc.201800161

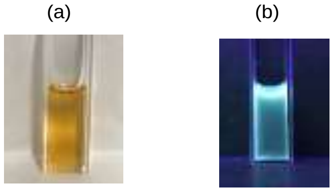

Figure 1. Photographs of (a) a solution of DMF-protected Fe_2O_3 NPs and (b) Light emitted by DMF-protected Fe_2O_3 NPs under black light irradiation (365 nm)

There are recent reports with iron oxide nanocatalysts in various organic reactions.[18]

We report structural characterization of Fe_2O_3 NPs synthesized using the DMF reduction method, and a novel recyclable catalytic system for hydrosilylation of alkenes without any additives.

The DMF-stabilized iron nanoparticles were prepared using a facile one step process. DMF (50 mL) was preheated to 140 °C in a flask fitted with a reflux condenser, and a solution of $Fe(acac)_3$ in DMF (0.5 mL, 0.1 M) was added. The DMF solution was heated at 140 °C for 8 h under open air conditions, after which highly dispersed iron nanoparticles were obtained. The iron nanoparticles in DMF resulted in an orange solution, which exhibited light-blue fluorescence when irradiated with black light (365 nm) (Fig. 1).

The spectroscopic properties of the iron nanoparticles were studied by UV-visible absorption and fluorescence spectroscopies. The maximum absorption peak was observed around 450 nm with UV excitation at 350 nm (Fig. S1). These results demonstrated similar photoluminescence to other metal nanoparticles synthesized using the DMF reduction method.[17]

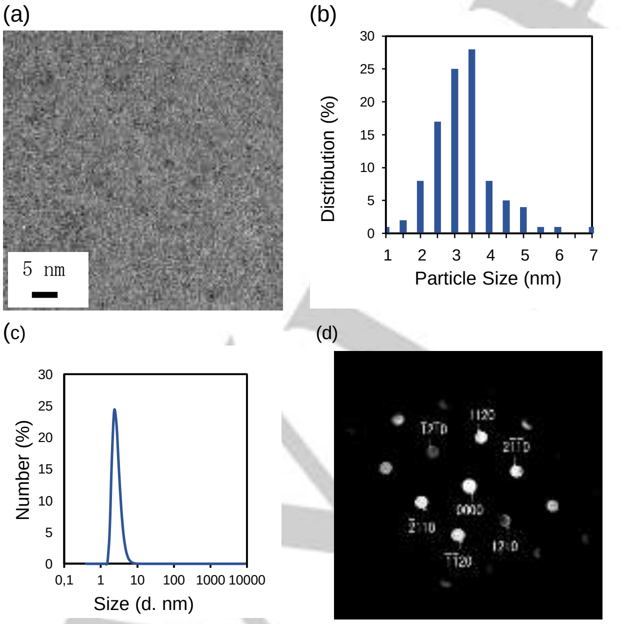

Figure 2. (a) Transmission electron microscopy image of DMF-protected Fe_2O_3 NPs; (b) particle size distribution of Fe_2O_3 NPs; (c) dynamic light scattering of Fe_2O_3 NPs; (d) electron diffraction pattern of Fe_2O_3 NPs.

To establish the size of the Fe_2O_3 nanoparticles, transmission electron microscopy (TEM) and dynamic light scattering (DLS) measurements were carried out. The TEM image and particle size distribution indicated that particles were mainly 2–5 nm in size (Fig. 2a and 2b). And results of DLS measurement showed the average particle size was 2.8 nm, which supports the TEM findings (Fig. 2c). The presence of iron in the metal nanoparticles was confirmed by energy dispersive X-ray spectroscopy (EDS; Fig. S2) and their crystalline structure were identified as α-Fe_2O_3 (corundum type) by electron diffraction analysis (Fig. 2d).[19]

To establish the crystal structure of all NP phases, X-ray diffraction (XRD) was carried out. The results revealed an amorphous structure (Fig. S3).

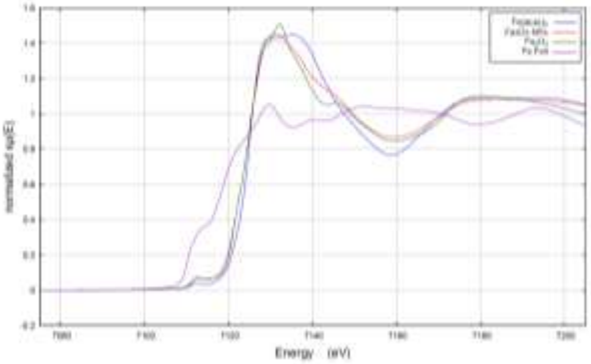

Figure 3. In situ Fe K edge X-ray absorptoion near-edge structure (XANES) spectra of Fe_2O_3 NPs, α-Fe_2O_3, $Fe(acac)_3$ and Fe foil. Cell Length 2.0-3.5 mm. Concentration 250 mM (for Fe_2O_3 NPs). (BL01B1 beamline at Spring 8 (Hyogo, Japan) in transmission QXAFS mode.)

Figure 3 shows an X-ray absorption near-edge structure (XANES) spectrum of DMF-protected iron NPs along with the spectra of α-Fe_2O_3, $Fe(acac)_3$ and Fe foil. The iron NP spectrum exhibited different absorption peaks to that of the $Fe(acac)_3$ precursor and almost overlapped with the α-Fe_2O_3 spectrum, supporting the finding that DMF-protected iron NPs had a similar structure to α-Fe_2O_3.

To gain an understanding of the interaction between DMF molecules and the Fe_2O_3 NPs, the catalyst was characterized by FT-IR, ^1H-NMR and X-ray photoelectron spectroscopies. Excess DMF solvent was removed using a high-vacuum pump (10^{-5} Pa) to ensure measurements were representative of the NPs. Figure S4 shows FT-IR spectra of DMF and Fe_2O_3 NPs. A strong peak at around 1670 cm^{-1}, attributed to the ν(C=O) stretching vibration of DMF, was observed in both spectra, which indicates the presence of DMF molecules on Fe_2O_3 NPs. In the ^1H-NMR spectrum of Fe_2O_3 NPs, the signal at 8.11 ppm, close to the formyl proton resonance of DMF at 7.92 ppm, indicates the interaction of DMF molecules with Fe_2O_3 NPs (Fig. S5). XPS spectra at Fe2p region of Fe_2O_3 and Fe_2O_3 NPs were presented in Figure 4. The curve fitting of their peaks indicated Fe^{2+} and Fe^{3+} states.[20a] At $Fe2p_{3/2}$ level of Fe_2O_3, the peaks located at 709.9 eV and 711.4 eV were assigned $2p_{3/2}$ of Fe^{2+} and

10.1002/cctc.201800161

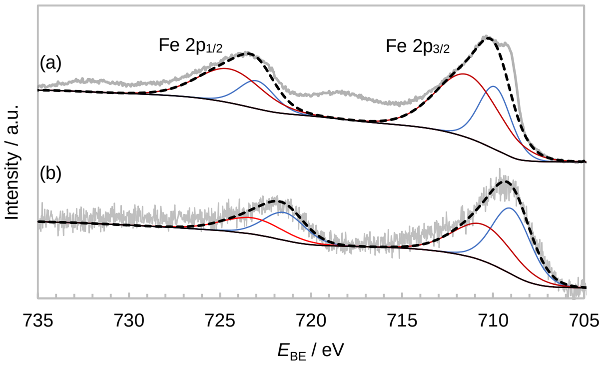

Figure 4. XPS spectra of Fe2p: (a) Fe_2O_3 and (b) Fe_2O_3 NPs.

Fe^{3+} states respectively and Fe^{2+}/ Fe^{3+} peak area ratio was 0.5 (Fig. 4a, Table S1). A Fe2p$_{3/2}$ spectrum of Fe_2O_3 NPs (Fig. 4b) was deconvoluted into two peaks at 709.2 eV and 710.9 eV, were considerably overlapped the peaks of Fe_2O_3. However Fe^{2+}/ Fe^{3+} peak area ratio of Fe2p spectrum for Fe_2O_3 NPs was 1.2, indicated more presence of Fe^{2+} species rather than bulk Fe_2O_3 , which attributed to coordination of DMF to the NPs (Table S1). To compare the chemical composition of Fe_2O_3 NPs with Fe_2O_3, XPS wide scan spectra were obtained (Fig. S6). Three principal peaks (C 1s, O 1s and N 1s) were observed and their narrow scan spectra were shown in Firgure S7. The N 1s peak was gained only the spectrum of Fe_2O_3 NPs, may be attributed to DMF. The O 1s peak at 532.3 eV (Fig. S7e) was also expected coordination of DMF to the NPs.[20b,c]

The thermal stability of Fe_2O_3 NPs was examined by thermo-gravimetric (TG) analysis (Fig. 5). The TG curve of the $Fe(acac)_3$ precursor showed a sharp drop off around 220 °C, whereas the weight loss of Fe_2O_3 NPs occurred gradually from 100 °C. The results suggested that the catalyst was different from the $Fe(acac)_3$ precursor because it was protected by DMF. To identify the protective molecules of the catalyst, evolved gas analysis-mass spectrometry (EGA-MS) was carried out (Fig. S8). At ~470 °C, NH_3 was released from Fe_2O_3 NPs and some ion fragments assigned *m/z* = 28 were observed at 570 °C and 710 °C. These ion fragments were expected to be N_2 or CO derived from decomposition products of DMF. [21]

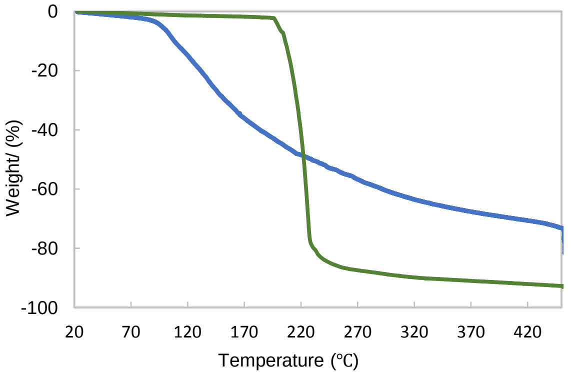

Figure 5. TG analysis of Fe_2O_3 NPs (blue) and $Fe(acac)_3$ (green).

Table 1: Fe_2O_3 NP-catalyzed hydrosilylation of alkenes with hydrosilane[a]

$$\underset{\mathbf{1}}{\textbf{Alkene}} + \underset{\mathbf{2}}{\textbf{Silane}} \xrightarrow{\textit{cat.}\ Fe_2O_3\ \text{NPs}} \underset{\mathbf{3}}{\textbf{Silylated product}}$$

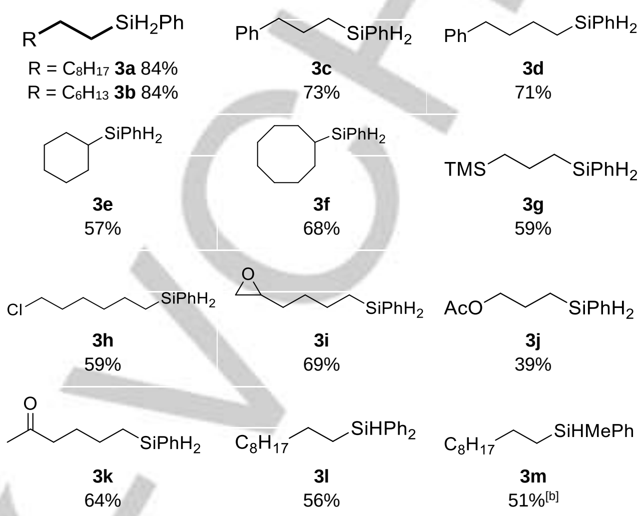

R = C_8H_{17} **3a** 84%
R = C_6H_{13} **3b** 84%
3c 73%
3d 71%
3e 57%
3f 68%
3g 59%
3h 59%
3i 69%
3j 39%
3k 64%
3l 56%
3m 51%[b]

[a] Reaction conditions: alkene **1** (0.5 mmol), hydrosilane **2** (3 mmol), Fe_2O_3 NPs (0.1 mol %), THF 1 mL, 70 °C, 24 h. [b] 48 h.

Following characterization, Fe_2O_3 NPs were used as a catalyst for hydrosilylation of alkenes (Table 1). Various alkenes were investigated by reaction with phenylsilane (**3a**–**3k**). 1-Decene was used as a model substrate for the catalytic system. The reaction proceeded smoothly and resulted in quantitative production of hydrosilylation product, with an isolated yield of 84% (**3a**) along with small amount of diphenylsilane. The use of excess amount of hydrosilane gave **3a** in high yield under these conditions (Table S2). A linear analogue of silylation product was also obtained in excellent yield (**3b**). Aliphatic olefins bearing phenyl groups were applied to the reaction and produced alternative silylation products in high yields (**3c**, **3d**). Cycloalkenes also showed good reactivity (**3e**, **3f**). The reaction also tolerated functionalized alkenes (**3g**–**3k**). Notably, the silylation selectively proceeded in the presence of carbonyl derivatives because the C=O group was unreactive (**3j**, **3k**). [10e] If allyl acetate is used for hydrosilylation, general platinum catalysts often form π-allyl intermediates and produce decarboxylation products. Secondary silanes could also be used, and corresponding products were obtained in moderate yields (**3l**, **3m**). However, the reaction was slow when tertiary silanes were used. The reaction is believed to proceed similar pathway reported in the literature.[6a,b]

The DMF-stabilized iron nanoparticle catalysts in this system could be effectively recycled using a convenient solvent extraction method. During catalyst regeneration, the

10.1002/cctc.201800161

Scheme 1. Recycling process for DMF-stabilized Fe_2O_3 NPs in the reaction of **1a** with **2a** under the same conditions as in Table 1

NPs in the DMF layer could be easily traced using UV monitoring. The catalyst does not require preactivation treatment for the next recycling step. Each cycle of the test was carried out as described in Scheme 1. Separation and recovery of the catalyst from the reaction mixture was simple, requiring only three steps to regenerate the catalyst for the subsequent run. After the reaction, the mixture was evaporated to remove the THF solvent. Hexane (8 mL) and DMF (2 mL) were then added and the catalyst was extracted with hexane five times to thoroughly remove reaction products and unreacted substrates. The catalyst remained well dispersed in the DMF layer (**A**), which could be observed by photoluminescence under black light irradiation. Finally, the DMF was evaporated to leave only iron nanoparticles (**B**). The subsequent run was conducted under the same conditions as described in Table 1 using the recovered catalyst. These processes were carried out in air, which demonstrated the stability of the Fe_2O_3 NP catalyst. The recycling test was performed five times. Black light irradiation confirmed that the Fe_2O_3 NP catalyst was present in the DMF phase, even in the last extraction following the 4th run, prior to the 5th run (Fig. S9). The recycling studies are shown in Figure 6. Fe_2O_3 NPs maintained their catalytic activity even after the 5th run, which resulted in silylation product in high yield. Slightly decreased of the yield of **3a** was observed during the multiple recycling step owing to the loss of some catalyst in the extraction step.

The catalyst retained their nano-sized particle size and showing similar photoluminescence characteristics before, after, and recycling reactions (Scheme 1, Figure 7 and S9-12). Therefore, DMF-stabilized Fe_2O_3 nanoparticles remain during the catalytic reaction, generating partially open sites by liberation a portion of the DMF molecules that could act as active catalysts in the reaction, as proposed in previously reported DMF-stabilized Ir and Cu nanoparticles.[17c,e] Even after the 5th run, the particle size was hardly changed (Fig. S11). If the first step of the recycling studies (THF elimination) was missed out, a red solution resembling bulk Fe_2O_3 was obtained after the final step (Scheme, S3). The NPs then showed no catalytic activity in the reaction. To understand the considerable loss of catalytic activity, the particle size was measured by DLS. This revealed a particle size of 74–79 nm (Fig. S13), which suggests that the preservation of particle size is important for successful catalytic reaction.

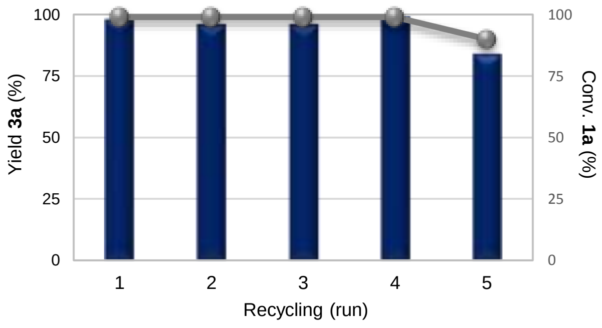

Figure 6. Recyclability studies of the Fe_2O_3 NP catalyst for hydrosilylation. Reactions were conducted under the same conditions as in Table 1.

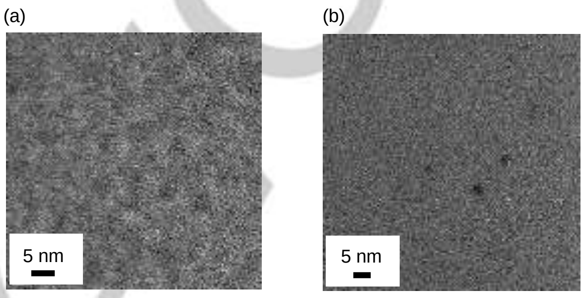

Figure 7. TEM images of Fe_2O_3 NPs (a) after reaction, (b) after the 5th run

In conclusion, we prepared DMF-protected iron NPs using a simple DMF reduction method and they were characterized as monodisperse α-Fe_2O_3 NPs (2‒5 nm) by TEM, DLS, electron diffraction, XANES, and XRD analyses. It was found that DMF molecules were present as a tightly bound protective layer around the Fe_2O_3 NPs, which affected their electronic interaction in FT-IR, ^{1}H-NMR, XPS, TG and EGA-MS analyses. The synthesized DMF-protected Fe_2O_3 NPs showed high catalytic activity for hydrosilylation of alkenes, resulting in versatile silylation products, without any additives. In addition, we proposed a simple, effective recycling process of the colloidal catalyst by extraction with a hexane-DMF system. No significant deactivation of the Fe_2O_3 NP catalyst was observed and particle retained their size, even after the 5th run. Further investigation into the detailed structure of the Fe-nanoparticle catalyst and its further application in catalysis are currently in progress.

Acknowledgements

This work was supported by the "Development of Innovative Catalytic Processes for Organosilicon Functional Materials“ project (PL: Kazuhiko Sato) from the New Energy and Industrial Technology Development Organization (NEDO). This work was also performed by Research Program of “Dynamic Alliance for Open Innovation Bridging Human, Environment and Materials and Devices“ and "the Cooperative Research Program of Institute for Catalysis, Hokkaido University (Grant 16B1005)“. We thank the members of the Comprehensive Analysis Center, SANKEN (ISIR), Osaka University for TEM, Global Facility Center, Hokkaido University for HRMS measurement, and Shimadzu Cooporation for EGA-MS analyses. The synchrotoron radiation experiments were performed at beamline BL01B1 of SPring-8 with the approval of the Japan Synchrotoron Radiation Research Institute (JASRI) (Proposal 2015B1246).

Keywords: iron nanoparticles • hydrosilylation • catalysis • *N*,*N*-dimethylformamide • catalyst recycle

[1] a) B. Su, Z. -C. Cao, Z. -J. Shi, *Acc. Chem. Res*., **2015**, *48*, 886-896; b) G. Pototschnig, N. Maulide, M. Schnürch, *Chem. Eur. J.*, **2017**, *23*, 9206-9232; c) E. A. Standley, S. Z. Tasker, K. L. Jensen, T. F. Jamison, *Acc. Chem. Res.*, **2015**, *48*, 1503-1514; d) J. Montgomery, *Acc. Chem. Res.*, **2000**, *33*, 467-473; e) M. Moselage, J. Li, L. Ackermann, *ACS catal.*, **2016**, *6*, 498-525.

[2] a) C. Bolm, J. Legros. J. L. Paih, L. Zani, *Chem. Rev.*, **2004**, *104*, 6217-6254; b) R. Shang, L. Ilies, E. Nakamura, *Chem. Rev.*, **2017**, *117*, 9086-9139; c) B. D. Sherry, A. Fürstner, *Acc. Chem. Res.*, **2008**, *41*, 1500-1511; d) S. -Y. Zhang, Y. -Q. Tu, C. -A. Fan, F. -M. Zhang, L. Shi, *Angew. Chem.*, **2009**, *121*, 8917-1921: *Angew. Chem. Int. Ed.*, **2009**, *48*, 8761-8765; e) C. -L. Sun, B. -J. Li, Z. -J. Shi, *Chem. Rev.*, **2011**, *111*, 1293-1314; f) F. Jia, Z. Li, *Org. Chem. Front.*, **2014**, *1*, 194-214.

[3] a) L. N. Lewis, J. Stein, Y. Gao, R. E. Colborn, G. Hutchins, *Plutinum Met. Rev.*, **1997**, *41*, 66-75; b) V. Compan, A. Andrio, A. L. -Alemany, E. Riande, M. F. Refojo, *Biomaterials*, **2002**, *23*, 2767-2772; c) L. V. Interrante, J. S. Rathore, *Dolton Trans*., **2010**, *39*, 9193-9202; d) M. Voronkov, N. Vlasova, Y. Pozhidaev, L. Belousova, O. Grigoryeva, *Polym. Adv.Technol.*, **2006**, *17*, 506-511.

[4] a) Y. Hatanaka, T. Hiyama, *J. Org. Chem.*, **1988**, *53*, 918-920; b) S. E. Denmark, C. S. Regens, *Acc. Chem. Res*, **2008**, *41*, 1486-1499; c) S. E. Denmark, J. H. C. Liu, *Angew. Chem.*, **2010**, *122*, 3040-3049; *Angew. Chem. Int. Ed.*, **2010**, *49*, 2978-2986; d) S. E. Denmark, M. H. Ober, *Adv. Synth. Catal.*, **2004**, *346*, 1703-1714.

[5] a) C. Cheng, J. F. Hartwig, *Chem. Rev.*, **2015**, *115*, 8946-8975; b) Y. Yang, C. Wang, *Sci. China. Chem.*, **2015**, *58*, 1266-1279; c) J. F. Hartwig, *Acc. Chem. Res.*, **2012**, *45*, 864-873.

[6] a) Y. Nakajima, S. Shimada, *RSC Adv.*, **2015**, *5*, 20603-20616; b) D. Troegel, J. Stohrer, *Coord. Chem. Rev.*, **2011**, *255*, 1440-1459; c) J. Sun, L. Deng, *ACS catal.*, **2016**, *6*, 290-300; d) X. Du, Z. Huang, *ACS catal.*, **2017**, *7*, 1227-1243.

[7] J. L. Speier, J. A. Webster, G. H. Barnes, *J. Am. Chem. Soc.*, **1957**, *79*, 974-979.

[8] B. D. Karstedt, General Electric Company, *US*3775452(A) **1973**.

[9] a) S. C. Bart, E. Labkovsky, P. J. Chirik, *J. Am. Chem. Soc.*, **2004**, *126*, 13794-13807; b) A. M. Tondreau, C. C. H. Atienza, K. J. Weller, S. A. Nye, K. M. Lewis, J. G. P. Delis, P. J. Chirick, Science, **2012**, *335*, 567-570.

[10] a) M. D. Greenhalgh, D. J. Frank, S. P. Thomas, *Adv. Synth. Catal.*, **2014**, *356*, 584-590; b) G. I. Nikonov, *Chemcatchem*, **2015**, *7*, 1918-1919; c) Y. Toya, K. Hayasaka, H. Nakazawa, *Organometallics*, **2017**, *36*, 1727-1735; d) X. Du, Y. Zhang, D. Peng, Z. Huang, *Angew. Chem.*, **2016**, *128*, 6783-6787; *Angew. Chem. Int. Ed.*, **2016**, *55*, 6671-6675; e) D. Peng, Y. Zhang, X. Du, L. Zhang, X. Leng, M. D. Welter, Z. Huang, *J. Am. Chem. Soc.*, **2013**, *135*, 19154-19166; f) L. Zhang, D. Peng, X. Leng. Z. Huang, *Angew. Chem.*, **2013**, *125*, 3764-3768; *Angew. Chem. Int. Ed.*, **2013**, *52*, 3676-3680; g) M. D. Greenhalgh, S. P. Thomas. *J. Am. Chem. Soc.*, **2012**, *134*, 11900-11903; h) E. Nakamura, N. Yoshikai, *J. Org. Chem.*, **2010**, *75*, 6061-6067; i) K. Kamata, A. Suzuki, Y. Nakai, H. Nakazawa, *Organometallics*, **2012**, *31*, 3825-3828; j) J. Chen, B. Cheng, M. Cao, Z. Lu, *Angew. Chem.*, **2015**, *127*, 4744-4747; *Angew. Chem. Int. Ed.*, **2015**, *54*, 4661-4664.

[11] a) Y. Sunada, D. Noda, H. Soejima, H. Tsutsumi, H. Nagashima, *Organometallics*, **2015**, *34*, 2896-2906; b) D. Noda, A. Tahara, Y. Sunada, H. Nagashima, *J. Am. Chem. Soc.*, **2016**, *138*, 2480-2483.

[12] a) A. J. Challinor, M. Calin, G. S. Nichol, N. B. Carter, S. P. Thomas, *Adv. Synth. Catal.*, **2016**, *358*, 2404-2409; b) C. Belger, B. Plietker, *Chem. Commun.*, **2012**, *48*, 5419-5421.

[13] I. Buslov, J. Becouse, S. Mazza, M. M. Clerc, X. Hu, *Angew. Chem.*, **2015**, *127*, 14731-14734; *Angew. Chem. Int. Ed.*, **2015**, *54*, 14523-14526.

[14] a) I. Chakraborty, T. Pradeep, *Chem. Rev*., **2017**, *117*, 8208-8271; b) A. Kumar, V. Kumar, *Chem. Rev.*, **2014**, *114*, 7044-7078.

[15] a) N. Yan, C. Xiao, Y. Kou, *Coord. Chem. Rev.*, **2010**, *254*, 1179-1218; b) D. Pla, M. Gómez, *ACS Catal.*, **2016**, *6*, 3537-3552; c) A. Bej, K. Ghosh, A. Sarkar, D. W. Knight, *RSC Adv.*, **2016**, *6*, 11446-11453; d) K. An, G. A. Somorjai, *ChemCatChem*, **2012**, *4*, 1512-1524; e) Y. Dai , Y. Wang , B. Liu , Y. Yang, *Small*, **2015**, *11*, 268-289.

[16] a) J. Lai, W. Niu, R. Luque, G. Xu, *Nano Today*, **2015**, *10*, 240-267; b) L. Zhang, W. Niu, G. Xu, *Nano Today*, **2012**, *7*, 586-605; c) A. Mirzaei, K. Janghorban, B. Hashemi, M. Bonyani, S. G. Leonardi, G. Neri, *Ceram. Int.*, **2016**, *42*, 6136-6144.

[17] a) M. Hyotanishi, Y. Isomura, H. Kawasaki, Y. Obora, *Chem. Commun.*, **2011**, *47*, 5750-5752; b) H. Yano, Y. Nakajima, Y. Obora, *J. Organomet. Chem.*, **2013**, *745*, 258-261; c) H. Oka, K. Kitai, T. Suzuki, Y. Obora, *RSC Adv.*, **2017**, *7*, 22869-22874; d) Y. Isomura, T. Narushima, H. Kawasaki, T. Yonezawa, Y. Obora, *Chem. Commun.*, **2012**, *48*, 3784-3786; e) K. Oikawa, S. Itoh, H. Kawasaki, Y. Obora, *Chem. Commun.*, **2017**, *53*, 1080-1083; f) H. Yamamoto, H. Yano, H. Kouchi, Y. Obora, R. Arakawa, H. Kawasaki, *Nanoscale*, **2012**, *4*, 4148-4154; g) X. Liu, C. Li, J. Xu, J. Lv, M. Zhu, Y. Guo, S. Cui, H. Liu, S. Wang, Y. Li, *J. Phys. Chem. C*, **2008**, *112*, 10778-10783; h) H. Kawasaki, H. Yamamoto, H. Fujimori, R. Arakawa, Y. Iwasaki, M. Inada, *Langmuir*, **2010**, *26*, 5926-5933; i) H. Kawasaki, H. Yamamoto, H. Fujimori, R. Arakawa, M. Inada, Y. Iwasaki. *Chem. Commun.*, **2010**, *46*, 3759-3761; j) M. Chiba, M. N. Thanh, Y. Hasegawa, Y. Obora, H. Kawasaki, T. Yonezawa, *J. Mater. Chem. C*, **2015**, *3*, 514-520.

[18] a) C. Wang, L. Salmon, R. Ciganda, L. Yate, S. Moya, J. Ruiz, D. Astruc, *Chem. Commun.*, **2017**, *53*, 644-646; b) X. Mou, X. Wei, Y. Li, W. Shen, *CrystEngComm*, **2012**, *14*, 5107-5120; c) F. Shi, M. K. Tse, M. -M. Pohl, J. Radnik, A. Brückner, S. Zhang, M. Beller, *J. Mol. Catal.*, **2008**, *292*, 28-35.

[19] M. Cao, T. Liu, S. Gao, G. Sun, X. Wu, C. Hu, Z. L. Wang, *Angew. Chem.*, **2005**, *117*, 4269-4273: *Angew. Chem. Int. Ed.*, **2005**, *44*, 4197-4201.

[20] a) R. L. Kurtz, V. E. Henrich, *Surf. Sci.*, **1983**, *129*, 345-354; b) Y. J. Kim, C. R. Park. *Inorg. Chem.*, **2002**, *41*, 6211-6216; c) T. Yamashita, P. Hayes, *Surf. Sci.*, **2008**, *254*, 2441-2449.

[21] J. Uchisawa, T. Nanba, S. Masukawa, A. Obuchi, Catal. Lett., 2004, 98, 103-106.

COMMUNICATION

Recyclable Fe nanoparticles hydrosilylation catalyst: Notable monodisperse iron nanoparticles (NPs) were synthesized by *N*,*N*-dimethylformamide (DMF) reduction method and their compositions were identified α-Fe_2O_3. The NPs served as an effective catalyst for alkene hydrosilylation, which gave versatile organosilicon compounds.

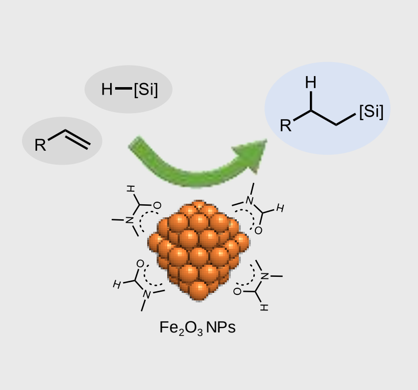

*Ryusei Azuma, Seiya Nakamichi, Jungo Kimura, Hiroki Yano, Hideya Kawasaki, Takeyuki Suzuki, Ryota Kondo, Yasuharu Kanda, Ken-ichi Shimizu, Kazuo Kato and Yasushi Obora**

Page No. – Page No.

Solution Synthesis of *N*,*N*-dimethylformamide-stabilized Iron Oxide Nanoparticles as an Efficient and Recyclable Catalyst for Alkene Hydrosilylation